Available online at www.sciencedirect.com

ScienceDirect

Procedia CIRP 116 (2023) 197–202

www.elsevier.com/locate/procedia

30th CIRP Life Cycle Engineering Conference.

# Development of a Polymer Spectral Database for Advanced Chemometric Analysis

Edward Ren Kai Neo[a,b,*], Jonathan Sze Choong Low[b], Vannessa Goodship[a], Stuart R.Coles[a], Kurt Debattista[a]

[a]*Warwick Manufacturing Group, University of Warwick, Coventry, CV4 7AL, United Kingdom*
[b]*Singapore Institute of Manufacturing Technology, 2 Fusionopolis Way, Singapore 138634, Singapore*

* Corresponding author. *E-mail address:* edward.neo@warwick.ac.uk

**Abstract**

The use of chemometric techniques with spectral data for sorting plastics to improve recycling rates have gained more attention in recent years. However, insufficient representation of polymer spectra in spectral databases has been one of the barriers to the further development of these techniques. This work aims to develop a polymer spectra dataset that builds upon existing spectral databases on two fronts. Firstly, the data collected includes Laser-induced Breakdown Spectroscopy (LIBS) data in addition to more commonly available Infrared (IR) and Raman data. Secondly, the dataset includes unaged and weathered conditions of the same sample. In total, the dataset includes 732 spectra, with the LIBS, IR and Raman spectra of 122 unique samples, both before and after accelerated weathering. The data collected were qualitatively analyzed and visualized. Further work will explore the effect of using hybrid spectroscopic methods on chemometrics analysis results.



*Keywords:* Chemometics; FTIR; Raman; LIBS; Plastic Recycling; Weathering

## 1. Introduction

The widespread use of plastic has led to plastic pollution globally, which has far-reaching environmental consequences on ecosystems and human health [1]. Recycling is generally accepted as the best end-of-life treatment for plastic waste [2]–[5], but the current global plastic recycling rate is only at around 18%. Nearly half of the plastic waste produced is mismanaged through end-of-life treatments like open dumping and open burning, particularly in less developed countries without proper waste management infrastructure [2], [6]. The factors contributing to such low recycling rates are multi-fold, including a mix of economic and technical challenges that vary across different countries [7], [8].

Proper sorting of plastic waste remains one of the greatest challenges for plastic recyclers across both economic and technical factors. It is technically very challenging to ensure tolerable contamination levels in sorted plastic streams in an economically viable fashion. Traditional sorting methods such as manual sorting or density sorting are labor intensive, resulting in high costs when scaled up at industrial levels. Furthermore, if the sorted plastic stream is contaminated with low quality plastic or other plastic types, the quality of the recycled plastic will be adversely affected, which severely diminishes the economic value of the recycled plastic as compared to virgin plastic [9].

The use of spectroscopic methods in automated sorting plastic has gained traction in recent years, with potential for much higher sorting speeds and accuracy [10]. Industrially, Near-infrared (NIR) spectroscopy is often used due to the use of highly quick and sensitive Indium Gallium Arsenic (InGaAs)-based detectors [11]. However, it has become


10.1016/j.procir.2023.02.034

increasingly feasible to use other spectroscopic methods, with the development of high-speed spectrometer using Mid-infrared (MIR) [12], Raman [13] and Laser-induced Breakdown Spectroscopy (LIBS) [14]. This has spurred a range of literature exploring the chemometric analysis of plastic spectral data in recent years, using techniques such as Principal Component Analysis (PCA), Partial Least Square (PLS), k-Nearest Neighbor (KNN), Support Vector Machine (SVM) and Artificial Neural Networks (ANN), all of which have yielded high accuracy in classifying various plastic types. These have been extensively discussed in various review articles [15]–[17].

Despite the promising results presented in the literature, there remains gaps in the field [15]. The spectral data used in some of the works tend to be homogeneous, involving only one sample per plastic type and does not include sufficient representation of weathered plastic samples as well. This may not be fully representative of the general postconsumer plastic waste mix received at recycling plants; hence the literature results may not translate well on an industrial level. The use of multi-modal spectroscopic methods has also not been explored. Since each of the spectroscopic methods have their own advantages and disadvantages, combining them may offer improvements in plastic sorting efficiency.

This paper details the development and analysis of a comprehensive plastic spectral database that could contribute towards overcoming the gap. The spectral database contains IR, Raman and LIBS data for each sample, covering a range of samples across each plastic type. The data spread within the collected spectral data were qualitatively analyzed. This database can be used for advanced chemometric analysis with techniques like deep learning in the future.

## 2. Methodology

### *2.1 Sample Preparation*

A total of 122 unaged plastics packaging samples till date across a range of colors were either bought or collected from postconsumer recyclable waste. The plastic samples had an even distribution of clear and opaque samples, with 57 clear samples and 65 opaque samples. plastic samples were comprised of the four most widely recyclable types – high density polyethylene (HDPE), low density polyethylene (LDPE), polypropylene (PP) and polyethylene terephthalate (PET), with the respective sample sizes and color variety listed in Table 1. The plastic types were identified from the Resin Identification Codes printed on the sample (1 for PET, 2 for HDPE, 4 for LDPE, 5 for PP) if present, otherwise FTIR spectroscopy was used to identify the plastic type. All the samples were cleaned thoroughly with water and detergent prior to analysis, then cut into sizes of approximately 30 x 50 mm for spectrum collection.

To simulate the effect of environmental degradation, each of the 122 samples was also subjected to accelerated weathering using a QUV/se accelerated weathering tester (Q-Lab, Cleveland USA). The samples were subjected to a cycle of UV irradiation with a UVA-340 lamp at 0.75 W/m2@ 340 nm at 60$^{o}$C for 4 hours, followed by a condensation cycle at 50$^{o}$C for another 4 hours over a period of up to four weeks. The samples were monitored weekly and were removed from accelerated weathering exposure before the full four weeks duration once there was noticeable loss in structural integrity.

Table 1. Respective sample size for each plastic type

| Plastic Type | Sample Size | Color Variety |
|---|---|---|
| HDPE | 26 | Clear, White, Black, Grey, Blue, Yellow, Green, Orange, Purple, Brown |
| LDPE | 17 | Clear, White, Black, Red, Green, Orange |
| PP | 40 | Clear, White, Black, Grey, Red, Blue, Yellow, Green, Purple, Brown |
| PET | 39 | Clear, White, Black, Grey, Blue, Green, Brown, Pink |

### *2.2 Spectroscopic Measurements*

FTIR, Raman and LIBS data were collected for all 122 samples both before and after accelerated weathering and curated into a database. The following sub-sections detail the equipment specifications for each of the spectroscopic technique.

#### *2.2.1 FTIR Measurement*

A Thermo Fisher Scientific Nicolet iN10 MX infrared microscope with a Germanium micro-tip attenuated total reflectance (ATR) crystal, operated with the OMNIC™ Picta™ software was used. The spectral range collected was from 675 – 4000 cm$^{-1}$, with 32 scans per sample at a resolution of 4 cm$^{-1}$. Background scans were conducted before each spectrum collection. The data was collected using a cooled MCT (mercury cadmium telluride) detector in absorbance mode.

#### *2.2.2 Raman Measurement*

A Renishaw InVia confocal Raman microscope with a NIR laser at 785nm operated with the WiRE 3.4 software was used. Initially, Raman data was also collected at 532nm and 633nm, but the 785mm laser wavelength was eventually chosen over other wavelengths as it reduced the effect of fluorescence [18], particularly in PET samples, without overly compromising the peak intensities for other plastic types. The spectral range collected was from 500 – 3200 cm$^{-1}$. All data were collected with a laser power of 30mW, x20 objective and a grating of 1200 l/mm, and was acquired for 10 second acquisition time.

#### *2.2.3 LIBS Measurement*

A SciAps Z-300 handheld LIBS analyzer with a laser at 1064nm, pulse energy of 7.5 mJ and pulse repetition rate of

50 Hz, operated with the Profile Builder software was used. The spectral range collected was 180 – 960 nm. The data was collected in an argon environment created using an internal miniature Argon tank. For each sample, the average of four spectra collected at four different points was collected, with a cleaning shot done before each spectrum acquisition.

### *2.3 Data Processing*

All raw spectra across the three data types were pre-processed with standard normal variate, asymmetric square baseline correction and Savitzky-Golay smoothing (window size 9 and third order polynomial), to remove noise from the spectral data and background fluorescence in the Raman spectrum [19].

### *2.4 Data Analysis*

Data analysis was done through Principal Component Analysis (PCA), a commonly used dimensionality reduction tool for chemometric analysis [20]. PCA constructs new axes known as principal components (PC) to maximize the variance in the dataset, hence capturing as much information as possible within each PC. The contribution of each PC to the overall data variance is represented by the explained variance ratio, which would collectively sum to a total of 1. By plotting the principal components with the highest explained variance ratios in a graph, the data distribution can be easily visualized and analyzed. PCA was performed for each of the three individual spectra type (FTIR, Raman, LIBS) using the Python scikit-learn library. Three components were extracted for analysis as the cumulative explained variance exceeded the threshold of 0.850.

## 3. Results and Discussion

This section will focus on the analysis of each type of spectral data in sub-sections 3.1-3.3. For each spectra type, PCA was used to qualitatively analyze 1) the extent of clustering for samples of the same plastic types and 2) the extent of differentiation between unaged and weathered samples of the same plastic type. A discussion of how all three types of spectra can be combined in a multi-modal approach is then presented in sub-section 3.4.

### *3.1 FTIR Data Analysis*

The average FTIR spectra of unaged and weathered plastic are presented in Figure 1a, while the PCA plot is presented in Figure 1b. The three principal components, PC1 – PC3 has a combined explained variance ratio sum of 0.904.

The PCA plot reveals clear differentiation between PE, PP and PET clusters, while HDPE and LDPE are quite closely clustered together due to their close chemical structure similarity. LDPE and PET form a much tighter cluster when compared to the HDPE and PP clusters, which points to the much more diverse range of HDPE and PP products in the market [21]. This is also reflected in the sample distribution within the dataset, as 64% of PET samples are colorless bottles or trays, while 50% of LDPE samples are colorless packaging films.

There is also some separation between unaged and weathered plastic samples, particularly for the HDPE, LDPE and PP, which appears to be mainly explained by PC3. Examining the FTIR spectra in Figure 1a, one of the key differences between unaged and weathered polyolefin samples is the presence of a ketone carbonyl peak at ~1712 $cm^{-1}$ formed during the photo-oxidation process, which is in agreement with previously reported literature [22], [23]. This is further supported by the loading plot for PC3, which reveals strong correlation at the carbonyl region. However, the unaged and weathered PET samples remain quite clustered in the PCA, as the FTIR spectra in Figure 1a shows limited differences between the unaged and weathered PET samples [19].

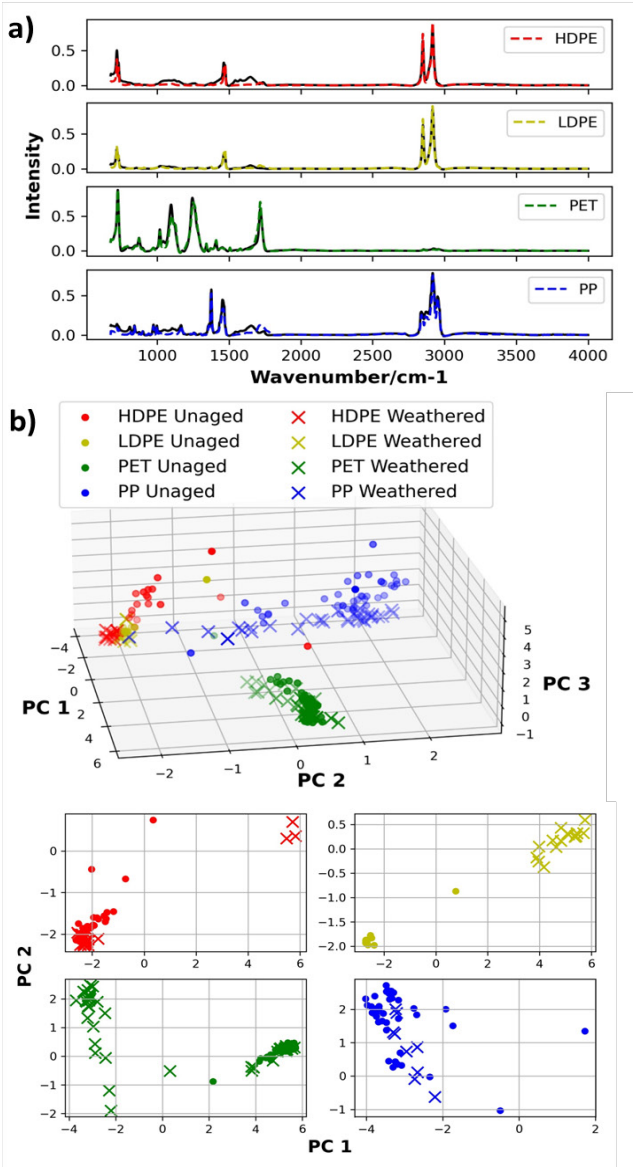


**Figure 1.** Qualitative Analysis of FTIR Spectra. (a) Plot of average unaged and weathered plastic spectrum. The unaged spectrum is represented by a black smooth line while the weathered spectrum is represented by a colored dotted line (b) PCA plot for FTIR spectra.

### 3.2 Raman Data Analysis

The average Raman spectra of unaged and weathered plastic and the PCA plot are presented in Figure 2a and 2b respectively. The three principal components, PC1 – PC3 has a combined explained variance ratio sum of 0.861.

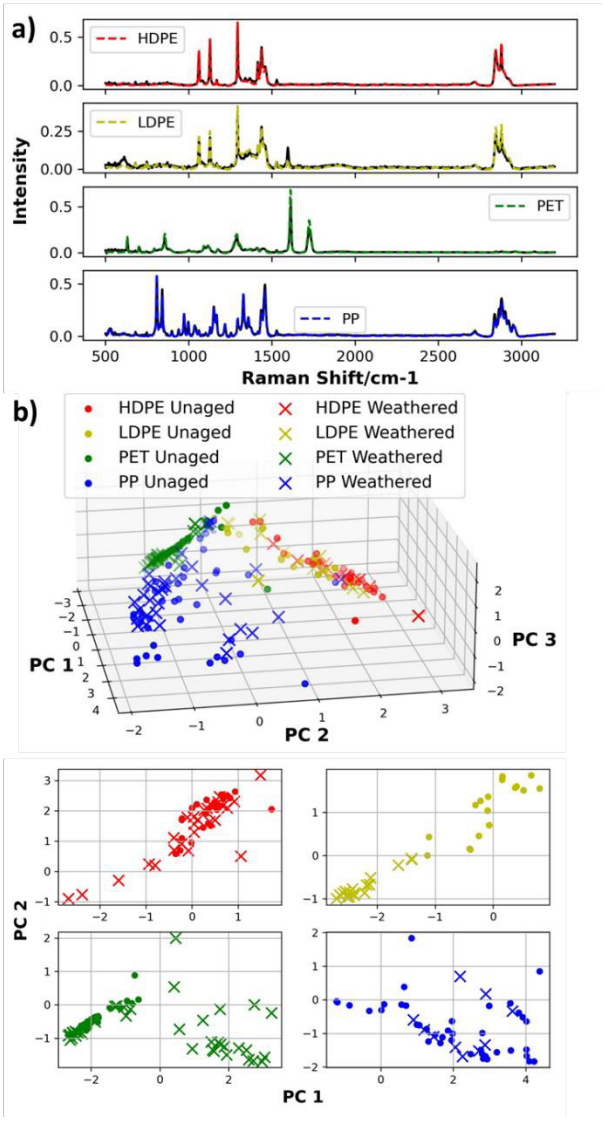


**Figure 2.** Qualitative Analysis of Raman Spectra. (a) Plot of average unaged and weathered plastic spectrum. The unaged spectrum is represented by a black smooth line while the weathered spectrum is represented by a colored dotted line (b) PCA plot for Raman spectra.

Similar to FTIR, the PCA plot for Raman spectra shows good separation between the different types of plastic. Most notably, there is much better differentiation between HDPE and LDPE, as changes in polymer crystallinity has been shown to correspond to changes in the Raman spectra [24]. This is evident in the Raman spectra plotted in Figure 2a, where HDPE much sharper $CH_2$ bending peaks at 1421 and 1445 $cm^{-1}$ [25].

However, the differentiation between unaged and weathered samples is much less distinct in the case of Raman, particularly for the polyolefins. This is due to a lack of carbonyl peaks present in the Raman spectra, a phenomenon that has been shown to occur with polymers as a result of overwhelming signals from long carbon chains [26]. In the case of PET, there appears to be a slight differentiation between unaged and weathered samples, but no clear differences can be observed between the Raman spectra of unaged and weathered samples.

### 3.3 LIBS Data Analysis

The average LIBS spectra of unaged and weathered plastic and the PCA plot are presented in Figure 3a and Figure 3b respectively. The three principal components, PC1 – PC3 has a combined explained variance ratio sum of 0.881

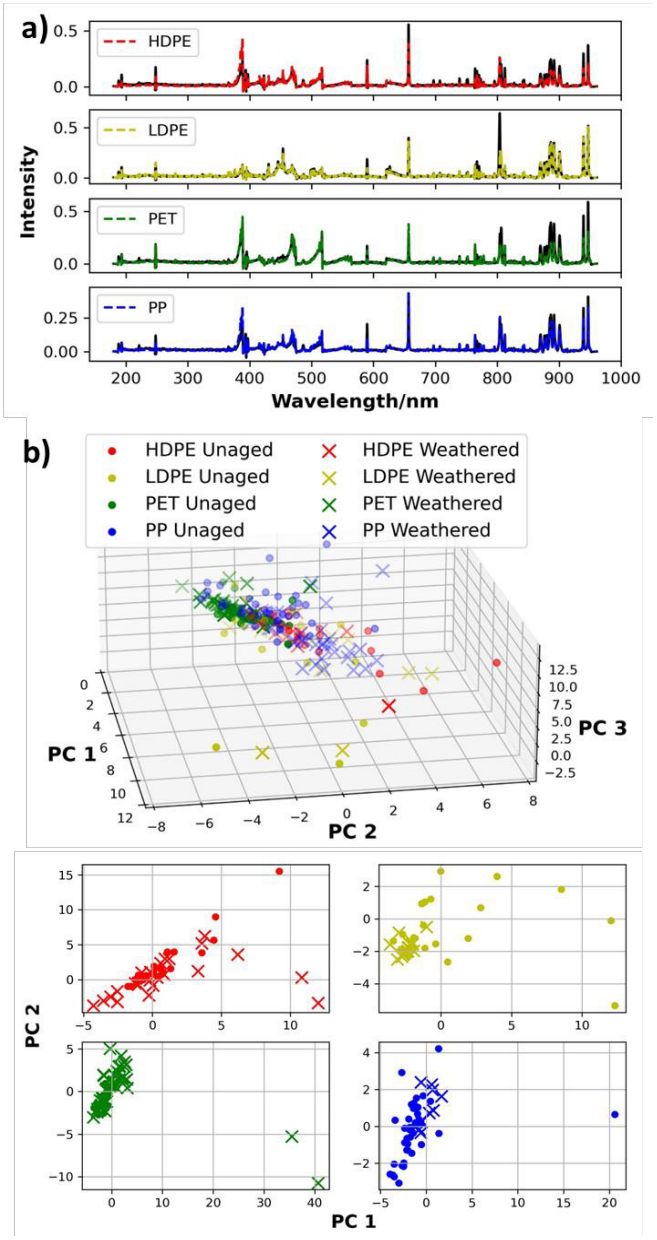


**Figure 3.** Qualitative Analysis of LIBS Spectra. (a) Plot of average unaged and weathered plastic spectrum. The unaged spectrum is represented by a black smooth line while the weathered spectrum is represented by a colored dotted line (b) PCA plot for LIBS spectra. Dots represent unaged samples while crosses represent weathered samples.

The PCA plot for LIBS spectra shows minimal clustering of each of the plastic type, with PET being the more distinct cluster. Since the plastics (particularly the polyolefins) have similar chemical compositions as long hydrocarbon chains, their corresponding LIBS profile are very similar, mainly just differing in the emission line intensities [27]. For instance, the polyolefins have a much higher C (247.85nm) to H (656.29nm) ratio as compared to PET, while PET has a stronger C2 band (512.96nm, 516.56nm) due to the presence of aromatic structure [28]. Most notably, this differs from some literature which previously reported good clustering of plastic LIBS data with PCA with multiple data points collected on the same sample, highlighting the effect of sample diversity on LIBS data.

While the LIBS PCA does not appear to give good class and weathering separation, a closer examination of the PCA loadings reveal that the PCs have a strong relationship with Ca emission lines at 393.33 and 396.88nm, which relates to calcium carbonate, a commonly used filler for polymers to improve polymer properties.

### *3.4 Discussion*

The data collected in this work has highlighted the challenges associated with sorting plastic in postconsumer waste, as there is a wide range of samples even within the same plastic type that results in spectral differences. However, qualitative analysis of the spectral data has shown that each type of spectra data can offer varying information. For instance, FTIR provided good separation between the plastic types (with the exception of HDPE and LDPE), and good separation between the unaged and weathered polyolefins. Raman was able to distinguish between HDPE and LDPE well, but not between unaged and weathered samples. LIBS generally gave poor separation between the plastic types, but could potentially identify the use of certain additives to determine the polymer properties.

A hybrid spectroscopic approach could be used to maximize the information contained with the three types of spectra. This could be achieved with multimodal deep learning, which involves the use of deep learning models to learn from information across different modalities [30]. Multimodal deep learning has found successful applications in different fields, such as the use of multiple imaging modalities for medical diagnosis, combination of multiple sensors for autonomous driving, emotion recognition from audio-visual inputs and automatic image/video captioning trained using visual and textual data [31], [32]. With the development of the polymer spectral database described in this work, multimodal deep learning for the sorting of plastic samples with FTIR, Raman and LIBS can be explored in the future. The pipeline for the future work would include two main phases: 1) Training of deep learning model and 2) Application in industry, both of which are in a feedback loop to each other. The framework for the pipeline is presented in Figure 4.

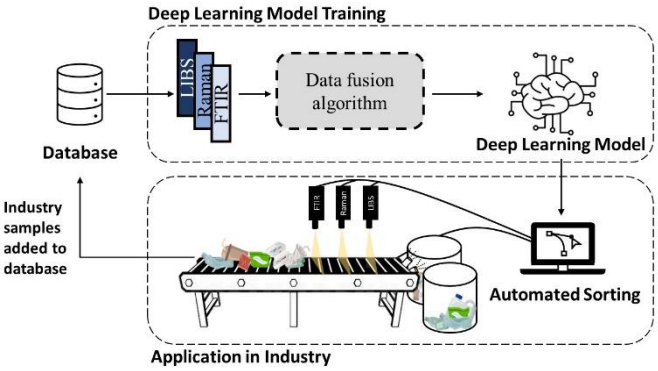


**Figure 4.** Framework for use of the multi-modal polymer spectral database.

The first phase involves the training of deep learning model using the FTIR, Raman and LIBS data in the database. A data fusion algorithm must first be applied to enable the deep learning to accept multi-modal data as input [33]. Subsequently, the trained deep learning model can then be applied on a sorting line with inline IR, Raman and LIBS spectrometer for data collection with unknown samples. The data collected is passed into the deep learning model for inference. Simultaneously, the data can be fed into the database, which can be used to improve the deep learning model.

## 4. Conclusion

In conclusion, the qualitative analysis of FTIR, Raman and LIBS data collected in this work has highlighted the potential of further exploring of a multi-modal approach. Further data collection can be done to build a more comprehensive and evenly distributed database with samples of higher variety of color and plastic types, which will help train a more robust deep learning model.

## Acknowledgements

The authors would like to thank Dr. Ben Breeze and the Spectroscopy RTP for technical support with FTIR and Raman spectrometer, Dr. Anwar Sattar and Dr. Jean Marshall for assistance with the LIBS spectrometer, Dr. Craig Carnegie and Ian Butterworth for assistance with the QUV.

## References

[1] J. R. Jambeck *et al.*, “Plastic waste inputs from land into the ocean,” *Science (80-. ).*, vol. 347, no. 6223, pp. 768–771, 2015.

[2] PEW Charitable Trusts; and SYSTEMIQ, “Breaking the Plastic Wave,” 2020. [Online]. Available: https://www.pewtrusts.org/-/media/assets/2020/07/breakingtheplasticwave_report.pdf.

[3] G. Faraca, V. Martinez-Sanchez, and T. F. Astrup, “Environmental life cycle cost assessment: Recycling of hard plastic waste collected at Danish recycling centres,” *Resour. Conserv. Recycl.*, vol. 143, pp. 299–309, 2019.

[4] Y. Chen *et al.*, “Life cycle assessment of end-of-life treatments of waste plastics in China,” *Resour. Conserv. Recycl.*, vol. 146, pp. 348–357, 2019, doi: https://doi.org/10.1016/j.resconrec.2019.03.011.

[5] E. R. K. Neo, G. C. Y. Soo, D. Z. L. Tan, K. Cady, K. T. Tong, and J. S. C. Low, “Life cycle assessment of plastic waste end-of-life for

India and Indonesia," *Resour. Conserv. Recycl.*, vol. 174, p. 105774, 2021, doi: https://doi.org/10.1016/j.resconrec.2021.105774.

[6] H. Ritchie, "Plastic Pollution," *Our World Data*, 2018, [Online]. Available: https://ourworldindata.org/plastic-pollution.

[7] S. Satapathy, "An analysis of barriers for plastic recycling in the Indian plastic industry," *Benchmarking*, vol. 24, no. 2, pp. 415–430, 2017, doi: 10.1108/BIJ-11-2014-0103.

[8] L. Milios, L. Holm Christensen, D. McKinnon, C. Christensen, M. K. Rasch, and M. Hallstrøm Eriksen, "Plastic recycling in the Nordics: A value chain market analysis," *Waste Manag.*, vol. 76, pp. 180–189, 2018, doi: https://doi.org/10.1016/j.wasman.2018.03.034.

[9] J. Hopewell, R. Dvorak, and E. Kosior, "Plastics recycling: challenges and opportunities," *Philos. Trans. R. Soc. B Biol. Sci.*, vol. 364, no. 1526, pp. 2115–2126, 2009.

[10] S. P. Gundupalli, S. Hait, and A. Thakur, "A review on automated sorting of source-separated municipal solid waste for recycling," *Waste Manag.*, vol. 60, pp. 56–74, 2017, doi: https://doi.org/10.1016/j.wasman.2016.09.015.

[11] W. Becker, K. Sachsenheimer, and M. Klemenz, "Detection of Black Plastics in the Middle Infrared Spectrum (MIR) Using Photon Up-Conversion Technique for Polymer Recycling Purposes," *Polymers* , vol. 9, no. 9. 2017, doi: 10.3390/polym9090435.

[12] Specim, "Specim FX50," 2020. https://www.specim.fi/wp-content/uploads/2020/03/Specim-FX50-Technical-Datasheet-02.pdf (accessed May 06, 2021).

[13] W. Musu, A. Tsuchida, H. Kawazumi, and N. Oka, "Application of PCA-SVM and ANN Techniques for Plastic Identification by Raman Spectroscopy," in *2019 1st International Conference on Cybernetics and Intelligent System (ICORIS)*, 2019, vol. 1, pp. 114–118, doi: 10.1109/ICORIS.2019.8874880.

[14] Ocean Insight, "SpeedSorter™ LIBS Sorting Sensor." https://www.oceaninsight.com/products/systems/sorting-systems/speedsorter/ (accessed Aug. 10, 2020).

[15] E. R. K. Neo, Z. Yeo, J. S. C. Low, V. Goodship, and K. Debattista, "A review on chemometric techniques with infrared, Raman and laser-induced breakdown spectroscopy for sorting plastic waste in the recycling industry," *Resour. Conserv. Recycl.*, vol. 180, p. 106217, 2022, doi: https://doi.org/10.1016/j.resconrec.2022.106217.

[16] U. K. Adarsh, V. B. Kartha, C. Santhosh, and V. K. Unnikrishnan, "Spectroscopy: A promising tool for plastic waste management," *TrAC Trends Anal. Chem.*, vol. 149, p. 116534, 2022, doi: https://doi.org/10.1016/j.trac.2022.116534.

[17] C. Araujo-Andrade *et al.*, "Review on the photonic techniques suitable for automatic monitoring of the composition of multi-materials wastes in view of their posterior recycling," *Waste Manag. Res.*, vol. 39, no. 5, pp. 631–651, Mar. 2021, doi: 10.1177/0734242X21997908.

[18] K. Munno, H. De Frond, B. O'Donnell, and C. M. Rochman, "Increasing the Accessibility for Characterizing Microplastics: Introducing New Application-Based and Spectral Libraries of Plastic Particles (SLoPP and SLoPP-E)," *Anal. Chem.*, vol. 92, no. 3, pp. 2443–2451, Feb. 2020, doi: 10.1021/acs.analchem.9b03626.

[19] M. Dong, Q. Zhang, X. Xing, W. Chen, Z. She, and Z. Luo, "Raman spectra and surface changes of microplastics weathered under natural environments," *Sci. Total Environ.*, vol. 739, p. 139990, 2020, doi: 10.1016/j.scitotenv.2020.139990.

[20] I. T. Jolliffe and J. Cadima, "Principal component analysis: a review and recent developments," *Philos. Trans. R. Soc. A Math. Phys. Eng. Sci.*, vol. 374, no. 2065, p. 20150202, Apr. 2016, doi: 10.1098/rsta.2015.0202.

[21] Plastindia Foundation, "Report on The Indian Plastics Industry," 2019. [Online]. Available: https://plastindia.org/pi-status-report-pdf.html#book/145.

[22] C. Signoret, A.-S. Caro-Bretelle, J.-M. Lopez-Cuesta, P. Ienny, and D. Perrin, "MIR spectral characterization of plastic to enable discrimination in an industrial recycling context: II. Specific case of polyolefins," *Waste Manag.*, vol. 98, pp. 160–172, 2019, doi: https://doi.org/10.1016/j.wasman.2019.08.010.

[23] M. Hamzah *et al.*, "Surface chemistry changes and microstructure evaluation of low density nanocluster polyethylene under natural weathering: A spectroscopic investigation," *J. Phys. Conf. Ser.*, vol. 984, p. 12010, 2018, doi: 10.1088/1742-6596/984/1/012010.

[24] B. H. Stuart, "Polymer crystallinity studied using Raman spectroscopy," *Vib. Spectrosc.*, vol. 10, no. 2, pp. 79–87, 1996, doi: https://doi.org/10.1016/0924-2031(95)00042-9.

[25] H. Sato *et al.*, "Raman spectra of high-density, low-density, and linear low-density polyethylene pellets and prediction of their physical properties by multivariate data analysis," *J. Appl. Polym. Sci.*, vol. 86, no. 2, pp. 443–448, Oct. 2002, doi: https://doi.org/10.1002/app.10999.

[26] C. Farber *et al.*, "Complementarity of Raman and Infrared Spectroscopy for Structural Characterization of Plant Epicuticular Waxes," *ACS Omega*, vol. 4, no. 2, pp. 3700–3707, Feb. 2019, doi: 10.1021/acsomega.8b03675.

[27] R. Junjuri and M. K. Gundawar, "A low-cost LIBS detection system combined with chemometrics for rapid identification of plastic waste," *Waste Manag.*, vol. 117, pp. 48–57, 2020, doi: https://doi.org/10.1016/j.wasman.2020.07.046.

[28] R. Junjuri and M. K. Gundawar, "Femtosecond laser-induced breakdown spectroscopy studies for the identification of plastics," *J. Anal. At. Spectrom.*, vol. 34, no. 8, pp. 1683–1692, 2019, doi: 10.1039/C9JA00102F.

[29] J. J. C. and L. D. S. and M. S. and L. J. J. and J. M. L. Poyato, "Optical Breakdown in Gases Induced by High-power IR CO2 Laser Pulses." Nova Science Publishers, 2011.

[30] J. Ngiam, A. Khosla, M. Kim, J. Nam, H. Lee, and A. Y. Ng, "Multimodal deep learning," 2011.

[31] K. Bayoudh, R. Knani, F. Hamdaoui, and A. Mtibaa, "A survey on deep multimodal learning for computer vision: advances, trends, applications, and datasets," *Vis. Comput.*, vol. 38, no. 8, pp. 2939–2970, 2022, doi: 10.1007/s00371-021-02166-7.

[32] J. Summaira, X. Li, A. M. Shoib, S. Li, and J. Abdul, "Recent Advances and Trends in Multimodal Deep Learning: A Review," *arXiv Prepr. arXiv2105.11087*, 2021.

[33] R. Bokade *et al.*, "A cross-disciplinary comparison of multimodal data fusion approaches and applications: Accelerating learning through trans-disciplinary information sharing," *Expert Syst. Appl.*, vol. 165, p. 113885, 2021, doi: https://doi.org/10.1016/j.eswa.2020.113885.